Solution of A Mass Transfer Based Mathematical Model of SCFE Process using COMSOL Multiphysics 5.2

[*]Bhupendra Suryawansi[1], Bikash Mohanty[2]

[1,2]Indian Institute of Technology, Roorkee , Uttarakhand (India) – 247667
*Corresponding author: Indian Institute of Technology, Roorkee, Uttarakhand (India) – 247667,
Email id: surya_bhupen@yahoo.com

Abstract: In the present work, COMSOL Multiphysics 5.2 was used to solve a mass transfer based mathematical model (Stastova et al., 1996) which is a modified form of Sovova H.,1994 model. The modification has been brought about by introducing the term 'Grinding efficiency' in the model and the results of the this model has been compared with the theoretical results obtained by Duba and Fiori, 2015 when the Stastova et al., 1996 model for SC-CO_2 extraction of grape seeds was solved using MATLAB. The model was validated for the SC-CO_2 extractions of grape seed at three temperatures (35, 40 and 50 ^oC), four pressures (200, 300, 400 and 500 bar), four flow rates-CO_2 (4.71, 7.45, 8.43 and 10.22 g/min), four particle sizes (0.41, 0.45, 0.59 and 0.75 mm) and four bed porosities (0.41, 0.32, 0.23 and 0.10). The model's mechanism is based on DDD (Desorption-Dissolution-Diffusion) phenomenon which is expressed by three analytic equations, representing three different regions of whole extraction curve. While using the COMSOL Multiphysics 5.2, an analytic function under the 'equation based modelling' was used to solve each mathematical equation and then the output results are combined. The results obtained through COMSOL Multiphysics 5.2 were compared with the results of Duba and Fiori, 2015 when the same model was solved using MATLAB within an error band % (-16.357 to +18.154%) and AARD band % (1.607 to 9.629%).The present results show good agreement with the results reported by Duba and Fiori, 2015.

Keywords: Supercritical fluid extraction, Grape seeds, Equation based modeling

1. Introduction

Supercritical fluid extraction (SFE) has been named as 'Green' technology due to its compatibility with the environment during the effective and efficient extraction of various plants products (i.e. Seeds, Leaves, Stems, Flowers, Roots, Fruits and Herbs). Now a day, it is being adopted in food, pharmaceutical, petroleum, cosmetic and other chemical industries with an aim to reduce organic solvent consumption and to achieve desired quality & quantity of solutes required for extraction so that environment pollution could be reduced significantly. In comparison to various solvents (n-Hexane, Ethanol, Methanol, Petroleum ether, Acetone etc.) that have been used for extraction, Carbon dioxide in its supercritical state (above its critical temperature (32 ^oC) and pressure (72 bar) has shown improved qualities such as; non-flammable, non-toxic, non-corrosive, non-reactive nature. Further, its solvent power may be enhanced by addition of modifiers (liquid compounds) of different polarities. It is one of the least expensive solvents after water. It does not leave any solvent residue after extraction. Carbon di-oxide is a relatively good solvent for non-polar solids and hydrocarbons.

Many mass transfer based mathematical models have been developed by a number of researchers for the SC-CO_2 extraction process to predict it kinetics and to scale-up this process at industrial level. A large number of kinetic models have been reported in the literature for the SC-CO_2 extraction processes. Amongst them, BIC (broken and intact cell) model proposed by Sovova (Sovova H., 1994) has been used most widely.

In the present work, the model proposed by Stastova (Stastova et al., 1996) which is a modified form of Sovova (Sovova H., 1994) model has been solved by COMSOL Multiphysics 5.2. The modification in the model has been brought about by inducting the term 'Grinding efficiency' in the model. The experimental conditions of parameters and calculated error % band, AARD % band are given in Table 1.

2. Mathematical modelling

The proposed model (Stastova et al., 1996) is based on differential mass balance in solid and solvent phase along the extraction bed as shown in Fig.1. It was assumed that part of the extractable seed material (x_p) is easily approachable to the solvent, due to the broken part of the cell structures which previously contained the solute, during the grinding of the raw material. On the other hand, the some part of the solute (x_k) remains

inside the structures of cell that were not broken by grinding.

P (bar)	200	300	400	500	Fixed parameters
	4.20 (y_s, mg/g)	7.60	10.4	13.0	T = 40 °C
	8.51 (Q, g/min)	8.43	8.32	8.59	ε_p = 0.41
	0.71 (G)	0.76	0.72	0.72	x_0 = 0.120
	1.2*10^{-2} ($k_f a_o$, 1/s)	9.8*10^{-3}	8.29*10^{-3}	6.61*10^{-3}	
	3.49*10^{-5} ($k_s a_o$, 1/s)	3.45*10^{-5}	7.18*10^{-5}	9.7*10^{-5}	**Error %** = -12.398 to +18.154
					AARD % = 7.26 to 9.629
T (°C)	**35**	**40**	**50**		**Fixed parameters**
	12.8 (y_s, mg/g)	13.0	13.4		P = 500 bar
	8.28 (Q, g/min)	8.59	8.70		ε_p = 0.41
	0.70 (G)	0.72	0.77		x_0 = 0.120
	3.02*10^{-3} ($k_f a_o$, 1/s)	6.61*10^{-3}	5.06*10^{-3}		
	6.44*10^{-5} ($k_s a_o$, 1/s)	9.7*10^{-5}	6.19*10^{-5}		**Error %** = -2.499 to +5.819
					AARD % = 2.252 to 3.049
Q (g/min)	**4.71**	**7.45**	**8.43**	**10.22**	**Fixed parameters**
	0.42 (d_p, mm)	0.43	0.41	0.43	T = 40 °C
	0.52 (G)	0.62	0.57	0.78	P = 350 bar
	3.84*10^{-3} ($k_f a_o$, 1/s)	6.98*10^{-3}	1.002*10^{-2}	1.27*10^{-2}	y_s = 8.60 mg/g
	2.3*10^{-5} ($k_s a_o$, 1/s)	5.04*10^{-5}	8.87*10^{-5}	9.73*10^{-5}	ε_p = 0.41
					x_0 = 0.120
					Error % = -16.357 to +17.813
					AARD % = 4.706 to 6.732
d_p (mm)	**0.41**	**0.45**	**0.59**	**0.75**	**Fixed parameters**
	7.34 (g/min)	7.19	7.46	7.31	T = 50 °C
	0.81 (G)	0.67	0.55	0.39	P = 500 bar
	3.26*10^{-3} ($k_f a_o$, 1/s)	4.27*10^{-3}	2.42*10^{-3}	6.11*10^{-3}	y_s = 13.4 mg/g
	4.98*10^{-5} ($k_s a_o$, 1/s)	2.44*10^{-5}	2.56*10^{-5}	1.98*10^{-5}	ε_p = 0.41
					x_0 = 0.167
					Error % = -1.351 to +15.733
					AARD % = 1.607 to 7.439
(ε_p)	**0.41**	**0.32**	**0.23**	**0.10**	**Fixed parameters**
	0.38 (d_p)	0.47	0.43	0.47	T = 50 °C
	8.84 (g/min)	8.38	8.63	8.43	P = 500 bar
	0.81 (G)	0.72	0.86	0.93	y_s = 13.4 mg/g
	6.33*10^{-3} ($k_f a_o$, 1/s)	4.87*10^{-3}	5.49*10^{-3}	1.77*10^{-3}	x_0 = 0.167
	9.63*10^{-5} ($k_s a_o$, 1/s)	1.14*10^{-4}	1.08*10^{-4}	2.33*10^{-5}	
					Error % = -1.451 to +5.912
					AARD % = 2.012 to 2.997

Table 1: Parametric conditions, estimated model parameters and calculated error % band for different operating parameters (P, T, Q, p, ep) during the SC-CO_2 extraction of grape seed oil.

The mass balance for a bed element where the height of the extraction bed is 'H' and the void fraction is 'ε'. The axial distance along the extraction bed is 'h'. The material balances on an element of extracting bed are reported by various researchers (Berna et al., 2000, Papamichail et al., 2000; Vasco et al., 2000) which were previously derived by Lack, 1985.

$$-\rho_s(1-\varepsilon)\frac{\partial x}{\partial t} = J(x,y) \qquad \ldots\ldots (1)$$

$$\rho_s(1-\varepsilon)\frac{\dot{Q}}{N}\frac{\partial y}{\partial h} = J(x,y) \qquad \ldots\ldots (2)$$

Assuming, 'solute free solvent' at the entrance of the extractor while all particles having uniform distribution of solute initially (x_0), the initial and boundary conditions are as follows;

$$x = x_0 \text{ at } t = 0 \text{ for } 0 \le h \le H \quad \text{and} \quad y = 0 \text{ at } h = 0 \text{ for } t \ge 0 \qquad \ldots\ldots (3)$$

The mass of solute extracted from the fixed bed is then defined as;

$$E = \dot{Q}\int_0^t y\,(h=1,t)\,dt \qquad \ldots\ldots (4)$$

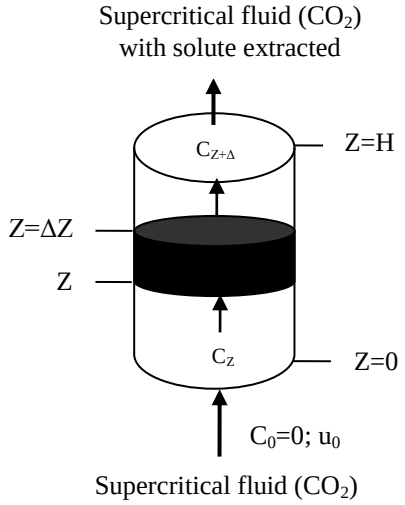

Fig.1: Schematic representation of extracting bed.

The mass transfer rate through this grinded part of seed is based on the fact that some part of 'solute' is already released during grinding. The easily approachable solute concentration in the solid phase is 'Gx_0' at the beginning point of extraction process. The rate of extraction in the first period of extraction process is controlled by its diffusion and convection in the solvent as;

$$J(x,y) = k_f a \rho_f (y_r - y) \quad for\ x > (1-G)x_0 \qquad \ldots\ldots (5)$$

The second period of extraction starts when the easily approachable solute has been removed. Then the extraction rate depends on the diffusion of solute from the interior of the seed particle to the surface. Now, the Eq. 5 was again simplified as;

$$J(x,y) = k_s a \rho_s (x - x^+) \quad for\ x \le (1-G)x_0 \qquad \ldots\ldots (6)$$

Equations (Eq.1 to Eq.6) were integrated numerically to obtain the mass of extract (Sovova H., 1994). Stastova (Stastova et al., 1996) applied a condition that k_s much less than k_f which says that in the second period 'y' much less than 'y_r' and x-x^+. Now the Eq.6 can be arranged as follows;

$$J = k_s a \rho_s (1 - y/y_r) \quad for\ x \le (1-G)x_0$$

..... (6a)

With the dimensionless time $\varphi = t.\dot{Q}y_r/(Nx_0)$

The mass of extract from Eq.1 – Eq.6 and Eq.6a for three different regions are given as follows;

For first period

$$E = Nx_0\varphi(1-\exp(-Z)) \qquad for\ \varphi \prec \frac{G}{Z} \quad \ldots\ldots (7)$$

For second period;

$$E = Nx_0(\varphi - \frac{G}{Z}\exp(Z(h_k - 1)))$$

$$for\ \frac{G}{Z} \le \varphi \prec \varphi_k \quad \ldots\ldots\ldots (8)$$

For third period;

$$E = Nx_0(1-\frac{1}{Y}\ln(1+(\exp(Y)-1)\exp(Y(\frac{G}{Z}-\varphi))(1-G)))$$

$$for\ \varphi \ge \varphi_k \quad \ldots\ldots\ldots (9)$$

Where;

$$\varphi_k = \frac{G}{Z} + \frac{1}{Y}\ln(1-G(1-\exp(Y)))$$

$$h_k = \frac{1}{Y}\ln(1+(\exp(Y(\varphi-\frac{G}{Z}))-1)/G) \qquad for\ \frac{G}{Z} \le \varphi \prec \varphi_k$$

$$Z = \frac{Nk_f a\rho_f}{\dot{Q}(1-\varepsilon)\rho_s} \quad and \quad Y = \frac{Nk_s a x_0}{\dot{Q}(1-\varepsilon)y_r}$$

Author solved this set of analytical equations by MATLAB and compared the results with experimental data.

3. Model solved by COMSOL Multiphysics 5.2

Model (Stastova et al., 1996) was solved using Model wizard of COMSOL Multiphysics 5.2 software. The method of solution is given in Appendix A. To solve this model, a 1D space dimension was chosen for under study option. After selecting model option, a Model Builder pop-up window appears. Parameters were given in option 'Parameters' under the Definitions as shown in Fig. A1. Now, since we have a set of analytic equations which have to be solved, three analytic functions (an1, an2, an3) were chosen in which all three analytic equations (Eq. 7, 8 & 9) were inserted with an argument ('t') which varies from lower limit to upper limit according to the conditions given to each equation and then created a plot of each equation as shown in Fig A2, A3, A4. After clicking 'create plot' of each equation , different functions (1D1, 1D1a, 1D1b) and three 1D plot groups (group1, group2, group3) appears as shown in Fig. A5 & A6 within the new data sets and different 1D plot groups respectively under the section 'Results' of the model builder. These three groups of pots were combined to get a complete nature of the model as shown in Fig. A7. Similarly, after putting the values of different operating conditions of parameters, estimated and adjustable model parameters and new solution could be achieved.

4. Results and discussions

Results obtained by solving model equations through COMSOL Multiphysics 5.2, were compared with the results reported by Duba and Fiori, 2015 in the literature as shown in Fig. (4a-4k). The effects of five parameters (pressure (200, 300, 400 and 500 bar), temperature (35, 40 and 50 ^{o}C), flow rate-CO_2 (4.71, 7.45, 8.43 and 10.22 g CO_2/min), particle size (0.41, 0.45, 0.59 and 0.75 mm) and particle bed porosity (0.41, 0.32, 0.23 and 0.10) on extraction yield (g oil/g seeds) versus solvent consumption (g CO_2/g seeds) were explained and compared the results when the same model was solved using MATLAB within an error % band ((-12.398 to +18.154), (-2.499 to +5.819), (-16.357 to +17.813), (-1.351 to +15.733) and (-1.451 to +5.912)) and absolute average relative deviation (AARD %) bands ((7.26 to 9.629), (2.252 to 3.049), (4.706 to 6.732), (1.607 to 7.439) and (2.012 to 2.997) respectively as reported in Table 1. From Fig. 4 (a, b), it is clear that increasing pressure has a positive effect on extraction yield and shows a wide range of error % band (-12.398 to +18.154). It may be due to an increase in pressure (at constant pressure) makes the density of SC-CO_2 increase which enhances its solvent power. The effect of extraction temperature during the SC-CO_2 The kinetic of extraction is rather conflicting due to a 'crossover phenomena' which explained that while increasing temperature, the density of SC-CO_2 decreases, but increased solute vapour pressure at higher temperature also causing the increase in solute solubility. The temperature's effect was studied at a pressure of 500 bar, which is above the upper crossover point. Solubility decreases between lower and upper crossover point with increases in temperature because the solvent density effect overcomes the vapour pressure effect and whereas below the lower or above the upper crossover point, the vapour pressure effect is more pronounced than the density effect, so the solubility increases with an increase in temperature as it can be seen in Fig. 4 (c, d). From the Fig. 4(e, f) it is clear that extraction yield increases with the increase of solvent flow rate but this has to be optimize in terms of extraction time and solvent volume used during

operation due to its wide range of error % band (-16.357 to +17.813). Fig. 4(g, h) show that the extraction yield decreases with the increase in particle size. It is also testified that at smaller particles the extraction yield approaches maximum yield ('0.14') which could not be reached by larger one because fine particles are having large 'surface area' per unit 'volume', containing a high percentage of free oil and require to cover less diffusional path for 'bound oil' to reach the surface which reduces the internal mass transfer resistance. The effect of different bed porosities on the extraction yield are resulted in Fig. 4(j, k) from which it is clear that for the bed porosity (0.23 to 0.41), initial extraction rate do not show significant effect while at bed porosity (0.10) it shows a negative effect. The negative effect may be due to channelling (causing flow inhomogeneity) resulting from high degree of compaction.

5. Conclusion

Results obtained through COMSOL Multiphysics 5.2 shows a good agreement with the MATLAB results found in literature with acceptable error % band and AARD % in each parametric condition. From the results it is clear that COMSOL Multiphysics 5.2 superior in terms of time consumption in computation and could be a better option to solve analytic equations.

6. References

1. Berna A., Tarrega A., Blasco M., Subirats S., Supercritical CO_2 Extraction of Essential Oil from Orange Peel; Effect of The Height of the Bed, *The Journal of Supercritical Fluids*, 18, 227-237 (2000).
2. Duba K.S., Fiori L., Supercritical CO_2 Extraction of Grape Seed Oil: Effect of Process Parameters on the Extraction Kinetics, *The Journal of Supercritical Fluids*, 98, 33-43 (2015).
3. Lack E. A., Criteria for the Design of Plants for the Supercritical Fluid Extraction of Natural Products, Ph.D. thesis , *TIJ Graz*, 1985.
4. Papamichail I., Louli V., Magoulas K., Supercritical Fluid Extraction of Celery Seed Oil, *The Journal of Supercritical Fluids*, 18, 213-226 (2000).
5. Sovova H., Rate of The Vegetable Oil Extraction With Supercritical CO_2-I. Modelling of Extraction Curves, *Chemical Engineering Science*, 49, 409-414 (1994).
6. Stastova J., Jez J., Bartlova M., Sovova H., Rate of the Vegetable Oil Extraction With Supercritical CO_2-III. Extraction from Sea Buckthorn, *Chemical Engineering Science*, 51, 4347 4352 (1996).

Vasco E.M.C.R., Coelho J.A.P., Palavra A.M.F., Marrone C., Reverchon E., Mathematical Modeling and Simulation of Pennyroyal Essential Oil Supercritical Extraction, *Chemical Engineering Science*, 55, 2917-2922 (2000).

7. Nomenclature

Symbol	Meaning
a :	Specific interfacial area
E:	Mass of extract
G:	Grinding efficiency $(0 \le G \le 1)$
H:	Axial co-ordinate $(0 \le h \le 1)$
J:	Mass transfer rate
K:	Mass transfer coefficient
N:	Solid feed
$\dot{Q}$:	Mass flow rate of solvent
t:	Time
U:	Superficial solvent velocity
v:	Interstitial solvent velocity
x:	Solid-phase concentration
x_0:	Initial concentration of solute in solid
y:	Solvent-phase concentration
y_r:	Solubility
Y:	Parameter of the second extraction period
Z:	Parameter of the first extraction period
ε :	Void fraction
ρ_f :	Solvent phase density
ρ_s :	Solid phase density
φ :	Dimensionless time
φ_k :	Dimensionless time
h_k:	Dimensionless co-ordinate
k_f:	Solvent phase mass transfer coefficient
k_s:	Solid phase mass transfer coefficient

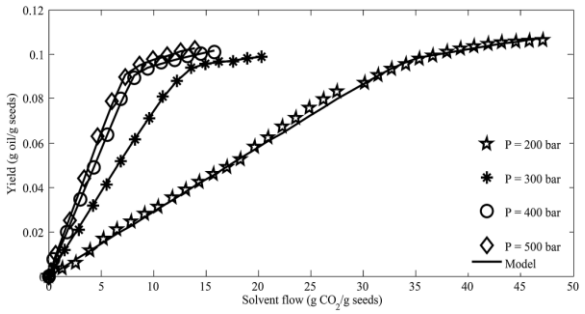

Fig. 4 (a). Solved through MATLAB

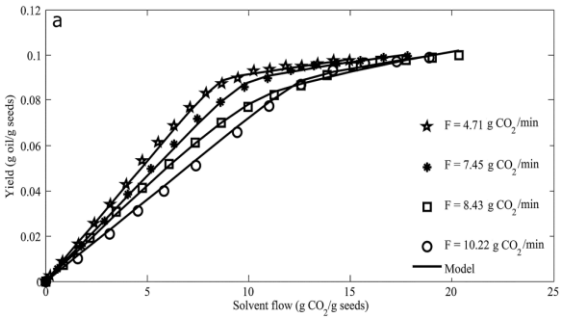

Fig. 4 (e). Solved through MATLAB

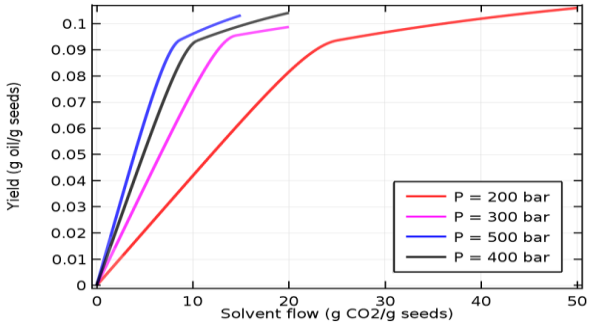

Fig. 4 (b). Solved through COMSOL

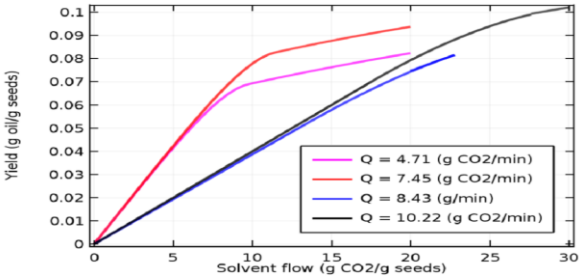

Fig. 4 (f) Solved through COMSOL

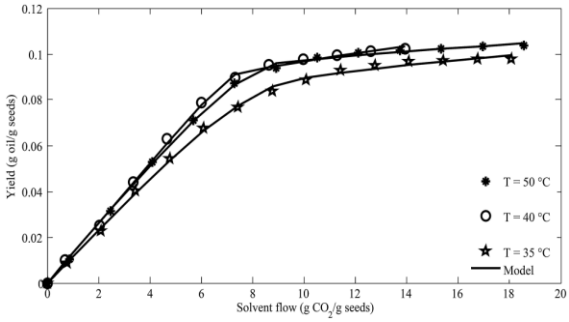

Fig. 4 (c). Solved through MATLAB

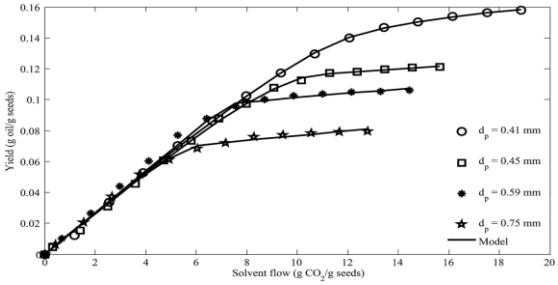

Fig. 4 (h). Solved through MATLAB

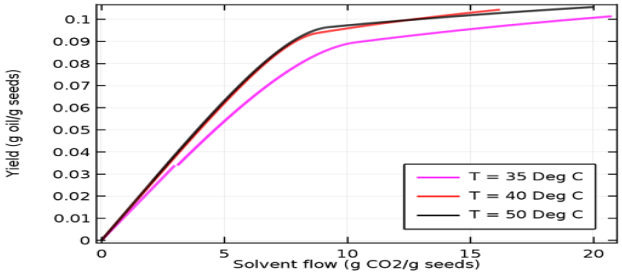

Fig. 4 (d). Solved through COMSOL

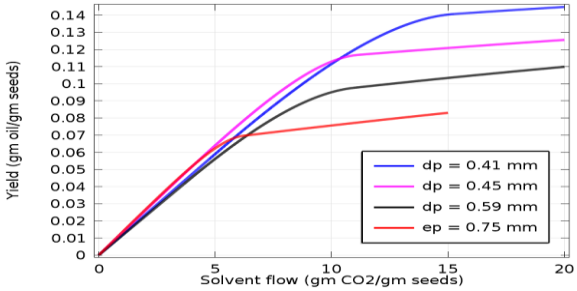

Fig. 4 (i) Solved through COMSOL

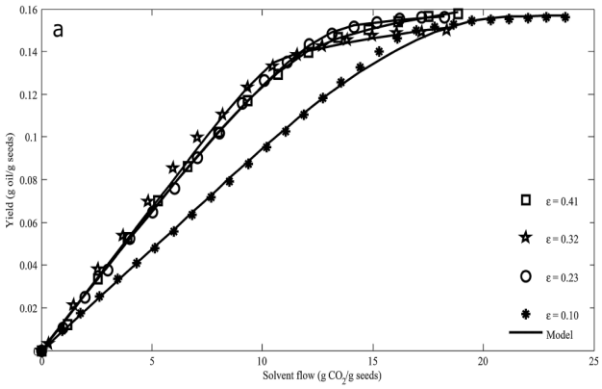

Fig. 4 (j) Solved through MATLAB

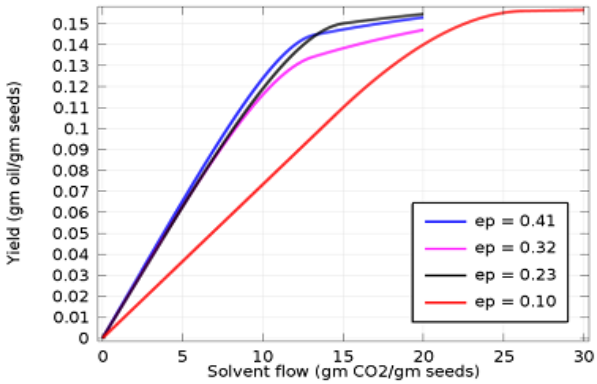

Fig. 4 (k). Solved through COMSOL

Appendix A

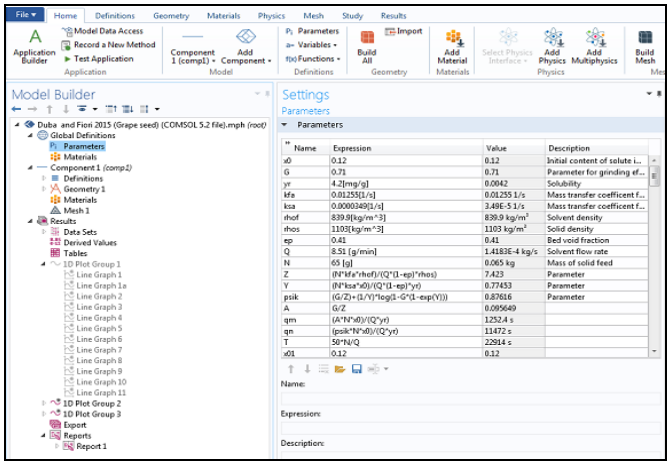

Fig. A 1: Model parameters setting window .

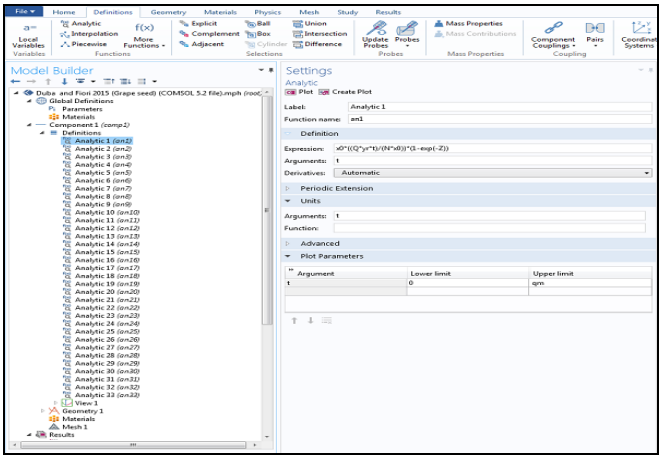

Fig. A2: Analytic equation-1 setting window of the model.

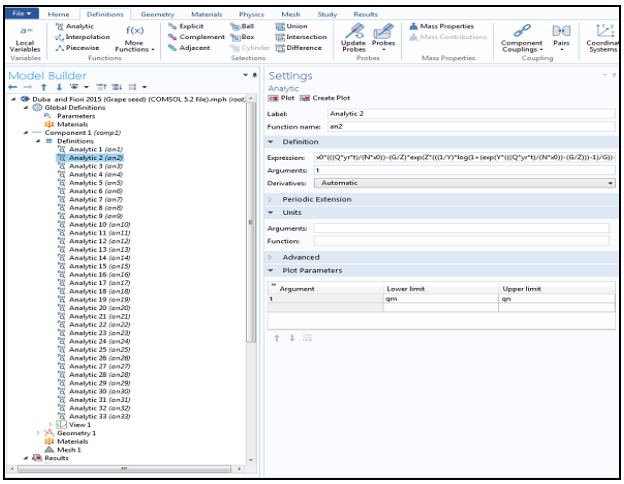

Fig.A3: Analytic equation-2 setting window of the model.

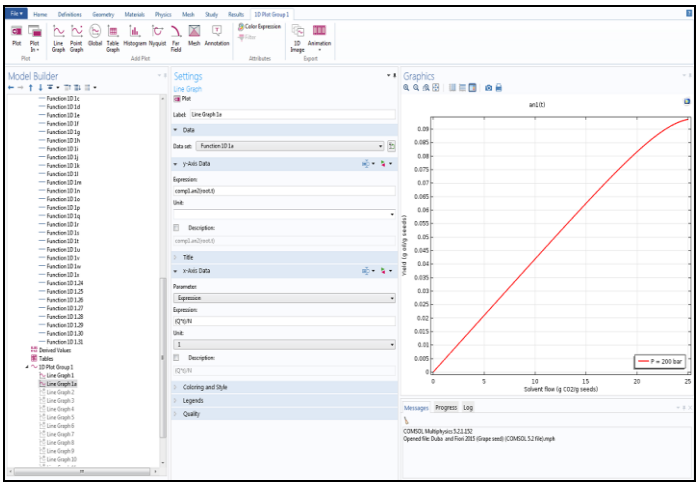

Fig.A6: Line graph of the analytic equations (Eq.1 & 2) window of the model.

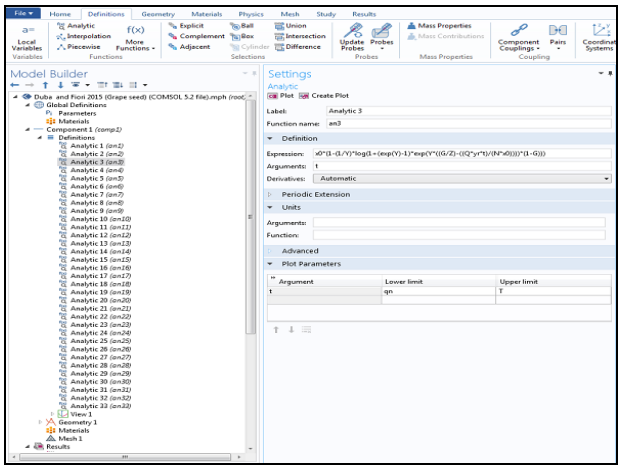

Fig.A4: Analytic equation-3 setting window of the model.

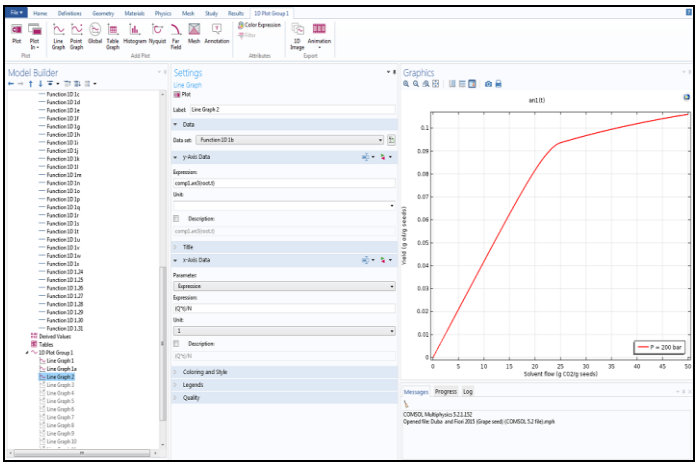

Fig.A7: A combined Line graph of the analytic equations (Eq.1, 2 & 3) window of the model.

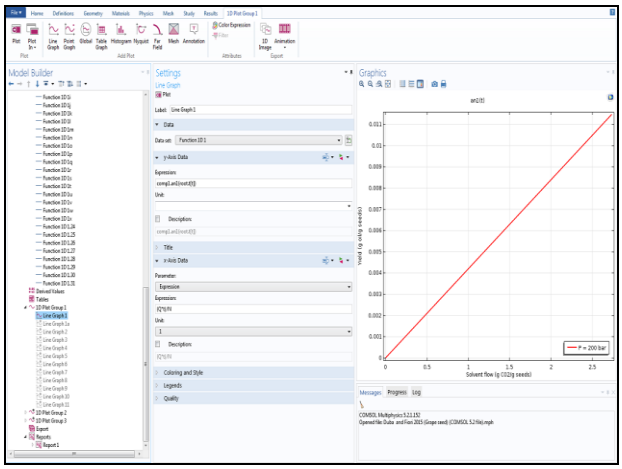

Fig.A5: Line graph of the analytic equation (Eq.1) window of the model.